

# SDSS-IV MaNGA: Non-Regular Rotators Quench Faster than Regular Rotators

R. J. Smethurst,<sup>1</sup> M. Merrifield,<sup>1</sup> K. L. Masters,<sup>2</sup> C. J. Lintott,<sup>3</sup>  
A.-M. Weijmans,<sup>4</sup> et al.

<sup>1</sup> *School of Physics and Astronomy, The University of Nottingham, University Park, Nottingham, NG7 2RD, UK*

<sup>2</sup> *Institute of Cosmology and Gravitation, University of Portsmouth, Dennis Sciama Building, Barnaby Road, Portsmouth, PO1 3FX, UK*

<sup>3</sup> *Oxford Astrophysics, Department of Physics, University of Oxford, Denys Wilkinson Building, Keble Road, Oxford, OX1 3RH, UK*

<sup>4</sup> *School of Physics and Astronomy, University of St Andrews, North Haugh, St Andrews, Fife, KY16 9RJ, UK*

5 May 2017

## ABSTRACT

With data from the MaNGA IFU survey, we classify 838 galaxies, which lie off the star forming sequence, as either regular or non-regular rotators and infer their exponentially declining star formation histories. We use  $u - r$  and  $NUV - u$  colours from SDSS and GALEX and a Bayesian method to infer the time and exponentially declining rate that quenching occurs in a galaxy. We find that across the non-regular rotator sample, quenching is more likely to occur at a rapid rate than across the regular rotator sample. The distribution of inferred quenching rates across the two samples is significantly ( $3\sigma$ ) different, suggesting that regular and non-regular rotators do indeed have different formation histories. We discuss how the total gas mass of a merger, rather than the merger mass ratio, may decide its ultimate kinematic fate.

**Key words:** galaxies – photometry, galaxies – statistics, galaxies – morphology

## 1 INTRODUCTION

Recent work studying the early-type galaxy population has revealed that it is actually composed of two separate populations. The majority of early-types are rotationally supported (Emsellem et al. 2011) with  $\sim 7$  times the number of regular (or ‘fast’) rotators, with kinematic discs, than non-regular (or ‘slow’) rotators, with dispersion dominated kinematics (Cappellari et al. 2007; Emsellem et al. 2007). This has led to the proposal of a revision of Hubble’s morphological classification scheme in the form of a ‘comb’ (Cappellari 2016), whereby the evolution of a galaxy, from disc to bulge-dominated, takes place along a ‘tine’ of the comb as a regular rotator, always retaining an underlying disc. If the discs of these regular rotators are somehow destroyed, they then evolve along the ‘handle’ of the comb to become non-regular rotators.

Dry major mergers are considered the most likely process to produce non-regular rotators (Duc et al. 2011; Naab et al. 2014) as they can rapidly destroy the disc dominated nature of a galaxy (Toomre & Toomre 1972). The percentage of non-regular rotators is therefore also an estimate for the fraction of the galaxy population which have undergone a dry major merger, approximated by previous works to be  $\sim 10 - 20\%$  since  $z \sim 1$ ; (Khochfar & Silk 2009).

Regular rotators, are thought to evolve from the slow build up of a galaxy’s bulge over time, eventually overwhelm-

ing the disc. This growth is thought to occur via gas-rich major or minor mergers (Duc et al. 2011) and gas accretion (Cappellari et al. 2013) which can produce a bulge dominated but rotationally supported galaxy (which would be visually classified as an early-type in the Hubble classification scheme). Although these mechanisms do not completely destroy the disc of a galaxy, they do cause an eventual morphological change from a pure disc to a visually bulge-dominated system.

If these two distinct populations of galaxies are formed by two different mechanisms, we should therefore also expect to find a difference in their star formation histories. Both major mergers and minor mergers have been postulated as quenching mechanisms (Mihos & Hernquist 1994; Hopkins et al. 2006, 2008a,b; Snyder et al. 2011; Hayward et al. 2014), with major mergers thought to cause a much faster quench of the remnant galaxy than a minor merger (Lotz et al. 2008, 2011). Gas accretion is also thought to cause quenching, as the large gravitational potential of the bulge that builds as the accreted gas sinks to the centre of the galaxy prevents the disc from collapsing and forming stars (Cheung et al. 2012; Fang et al. 2013).

In this work we use a Bayesian star formation inference package, STARPY to determine the quenching histories of a population of early-type galaxies, classified as either regular or non-regular rotators using data from the Mapping Nearby Galaxies at Apache (MaNGA) survey. We use broadband op-

tical,  $u-r$  and near-ultraviolet  $NUV-u$  colours from SDSS and GALEX to infer both the time and rate that quenching occurs in each galaxy, before visualising the distribution of these parameters across the regular and non-regular populations. We aim to determine whether regular and non-regular rotating galaxies quench at different rates.

This paper proceeds as follows. In Section 2 we describe our data sources and our Bayesian inference method for determining the quenching histories. We present our results in Section 3. We discuss the implications of our results in Section 4. The zero points of all magnitudes are in the AB system. Where necessary, we adopt the WMAP Seven-Year Cosmology (Jarosik et al. 2011) with  $(\Omega_m, \Omega_\Lambda, h) = (0.26, 0.73, 0.71)$ .

## 2 DATA AND METHODS

### 2.1 SDSS & GALEX Photometry

We obtain optical photometry from the Sloan Digital Sky Survey Data Release 7 (SDSS; York et al. 2000; Abazajian et al. 2009). We utilise the Petrosian magnitude, **petroMag**, values for the  $u$  (3543Å) and  $r$  (6231Å) wavebands provided by the SDSS DR7 pipeline (Stoughton et al. 2002). Further to this, we also required NUV (2267Å) photometry from the GALEX survey (Martin et al. 2005). Observed fluxes are corrected for galactic extinction (Oh et al. 2011) by applying the Cardelli, Clayton, & Mathis (1989) law. We also adopt  $k$ -corrections to  $z = 0.0$  and obtain absolute magnitudes from the NYU-VAGC (Blanton et al. 2005; Padmanabhan et al. 2008; Blanton & Roweis 2007).

### 2.2 MaNGA Survey & Data Reduction Pipeline

MaNGA is a multi-object IFU survey conducted with the 2.5 m Sloan Foundation Telescope (Gunn et al. 2006) at Apache Point Observatory (APO). By 2020 MaNGA will have acquired IFU spectroscopy for  $\sim 10000$  galaxies, all with  $M_* > 10^9 M_\odot$  and an approximately flat mass selection (Wake et al., in preparation). The target selection does not include any cuts on morphology, colour or environment.

In order to obtain spectra, MaNGA makes use of the Baryon Oscillation Spectroscopic Survey (BOSS) spectrograph (Smee et al. 2013). The BOSS spectrograph provides continuous coverage between 3600 Å and 10300 Å at a spectral resolution  $R \sim 2000$  ( $\sigma_{\text{instrument}} \sim 77 \text{ km s}^{-1}$ ).

Complete spectral coverage to  $1.5R_e$ , a galaxy’s effective radius, is obtained for the majority of targets, though a subset have coverage to  $2.5R_e$ . See Bundy et al. (2015) for an overview of the MaNGA survey. For a further description of the instrumentation used by MaNGA see Drory et al. (2015). For a detailed description of the observing strategy see Law et al. (2015) and for description of the survey design see Yan et al. (2016).

The raw data was processed by the MaNGA data reduction pipeline (DRP), which is discussed in detail Law et al. (2016). The MaNGA DRP extracts, wavelength calibrates and flux calibrates all fibre spectra obtained in every exposure. The individual fibre spectra are then used to form a regular gridded datacube of  $0.5''$  spaxels and spectral

channels. The spectra are logarithmically sampled with bin widths of  $\log \lambda = 10^{-4}$ .

These datacubes are then analysed using the MaNGA data analysis pipeline (DAP); the development of which is ongoing and will be described in detail in Westfall et al. (in preparation). The primary output from the DAP are the MAPS files which provide 2D “maps” (i.e., images) of DAP measured properties, which include flux, stellar-continuum fits, absorption- and emission-line properties and spectral index measurements. The DAP also provides a measurement of a galaxy’s effective radius,  $R_e$ , and the ellipticity within it,  $\epsilon_e$ , which is used along with the specific angular momentum to classify galaxies as either regular or non-regular rotators (see Section 2.3).

### 2.3 Data sample

There are currently 2,777 galaxies observed by the MaNGA survey and consequently part of SDSS DR7. We cross-matched these galaxies with a radius of  $3''$  to the GALEX survey in order to obtain NUV photometry (see Section 2.1), resulting in 1,413 galaxies. We shall refer to this as the MANGA-GALEX sample.

In this study we wish to study the quenching histories of these galaxies, therefore we sub-select those galaxies which are below the ‘star forming sequence’<sup>1</sup> (SFS). Here we utilise the values quoted in the MPA-JHU catalogue (Kauffmann et al. 2003; Brinchmann et al. 2004) wherein the SFR of a galaxy is quantified using the H $\alpha$  emission line observed in the SDSS fibre spectra and corrected for aperture bias using SDSS Petrosian photometry to provide a galaxy wide SFR. Whilst we do not use this value to infer the SFHs of these galaxies (see Section 2.4), we do utilise them to select a sample of galaxies with SFRs more than  $1\sigma$  below the SFS of Peng et al. (2010).

This selection on SFR when applied to the MANGA-GALEX sample results in a sample of 838 quenching or quenched galaxies, which we will refer to as the Q-MANGA-GALEX sample. The positions of these galaxies below the SFS are shown in Figure 1.

In order to classify the galaxies in the Q-MANGA-GALEX sample as regular rotators or otherwise, we use the equation for specific stellar angular momentum as defined by Emsellem et al. (2007, 2011);

$$\lambda_{R_e} = \frac{\sum_{i=1}^N F_i R_i |V_i|}{\sum_{i=1}^N F_i R_i (V_i^2 + \sigma_i^2)^{1/2}}, \quad (1)$$

where  $F_i$  is the flux in the  $i$ th spaxel,  $R_i$  the spaxel’s distance from the galaxy centre (where  $R_i < R_e$ , the effective radius of a galaxy),  $V_i$  the mean stellar velocity in that spaxel,  $\sigma_i$  the stellar velocity dispersion in that spaxel and  $N$  the total number of spaxels. In this work we use the python function provided in the MaNGA DAP to calculate  $\lambda_R$  using the values of mean flux, radius, stellar velocity and stellar velocity dispersion (corrected for instrumental resolution effects) provided in the MAPS files generated by the

<sup>1</sup> Sometimes referred to as the “main” sequence or star formation.

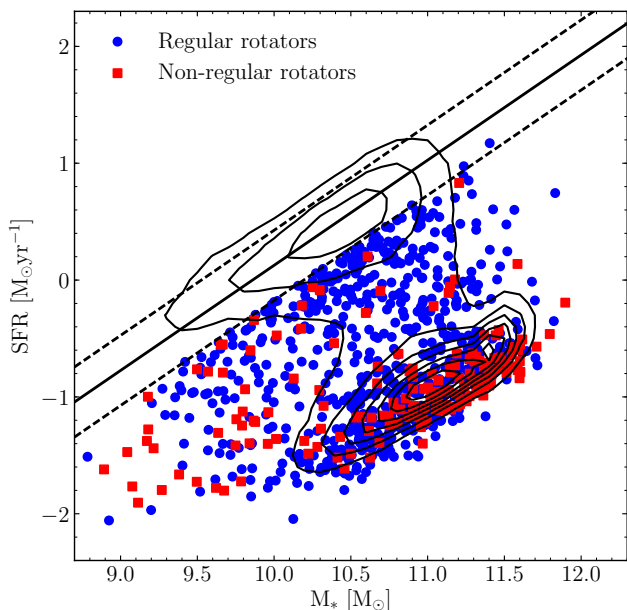


**Figure 1.** Stellar mass against star formation rate for the Q-MANGA-GALEX sample with regular (blue circles) and non-regular (red squares) rotators identified. Shown also are the contours for the entire MPA-JHU sample (black contours; i.e. SDSS DR7). The solid line shows the SFS as defined by Peng et al. (2010) at the average redshift of the Q-MANGA-GALEX sample with  $\pm 1\sigma$  shown by the dashed lines. Note that the galaxies in the Q-MANGA-GALEX sample are chosen to be more than  $1\sigma$  below the SFS as defined at their observed redshift and stellar mass (see Section 2.3).

MaNGA DAP (see Section 2.2). Velocity dispersion measurements in each spaxel of a galaxy were confirmed to be above the instrument resolution of  $77 \text{ km s}^{-1}$ .

We classify galaxies in the Q-MANGA-GALEX sample as regular or non-regular rotators using the definition from Cappellari (2016):

$$\lambda_{Re} < 0.08 + \frac{\epsilon_e}{4} \quad \text{with} \quad \epsilon_e < 0.4, \quad (2)$$

where  $\epsilon_e$  is the ellipticity of a galaxy within its effective radius,  $R_e$ . Using this definition reveals 673 (80%) regular rotators and 165 (20%) non-regular rotators in the Q-MANGA-GALEX sample. They are shown by their velocity maps in Figure 2 along with the definition of a non-regular rotator from Cappellari (2016), shown by the solid black line. This is a similar percentage of non-regular rotators as found by previous works (14–17% of early-types; Emsellem et al. 2011; Stott et al. 2016).

## 2.4 SFH Inference

STARPY<sup>2</sup> is a PYTHON code which allows the inference of the exponentially declining star formation history (SFH) of a single galaxy using Bayesian Markov Chain Monte Carlo techniques (Foreman-Mackey et al. 2013)<sup>3</sup>. The code uses the solar metallicity stellar population models of (Bruzual

& Charlot 2003, hereafter BC03), assumes a Chabrier IMF (Chabrier 2003) and requires the input of the observed  $u-r$  and  $NUV-u$  colours and redshift. No attempt is made to model for intrinsic dust.

The SFH is described by an exponentially declining SFR described by two parameters; the time at the onset of quenching,  $t_q$  [Gyr], and the exponential rate at which quenching occurs,  $\tau$  [Gyr]. Under the simplifying assumption that all galaxies formed at  $t = 0$  Gyr with an initial burst of star formation, the SFH can be described as:

$$SFR = \begin{cases} i_{sfr}(t_q) & \text{if } t < t_q \\ i_{sfr}(t_q) \times \exp\left(\frac{-(t-t_q)}{\tau}\right) & \text{if } t > t_q \end{cases} \quad (3)$$

where  $i_{sfr}$  is an initial constant star formation rate dependent on  $t_q$  (Schawinski et al. 2014; Smethurst et al. 2015). A smaller  $\tau$  value corresponds to a rapid quench, whereas a larger  $\tau$  value corresponds to a slower quench. Note that a galaxy undergoing a slow quench is not necessarily quiescent by the time of observation. Similarly, despite a rapid quenching rate, star formation in a galaxy may still be ongoing at very low rates, rather than being fully quenched. This SFH model has previously been shown to appropriately characterise quenching galaxies (Weiner et al. 2006; Martin et al. 2007; Noeske et al. 2007; Schawinski et al. 2014).

We assume a flat prior on all the model parameters and model the difference between the observed and predicted  $u-r$  and  $NUV-u$  colours as independent realisations of a double Gaussian likelihood function (Equation 2 in Smethurst et al. 2015). We also make the simplifying assumption that the age of each galaxy,  $t_{age}$  corresponds to the age of the Universe at its observed redshift,  $t_{obs}$ .

The probabilistic fitting methods to these star formation histories for an observed galaxy are described in full detail in Section 3.2 of Smethurst et al. (2015), wherein the STARPY code was used to characterise the morphologically dependence of the SFHs of  $\sim 126,000$  galaxies. Similarly, in Smethurst et al. (2016), STARPY was used to show the prevalence of rapid, recent quenching within a population of AGN host galaxies and in Smethurst et al. (2017) to investigate the quenching histories of group galaxies.

An example posterior probability distribution output by STARPY is shown for a single galaxy in Figure 5 of Smethurst et al. (2015), wherein the degeneracies of the SFH model between recent, rapid quenching and earlier, slower quenching can clearly be seen.

To study the SFH across a sample of many galaxies, these individual posterior probability distributions are stacked in  $[t_q, \tau]$  space to give a single distribution for the sample. This is no longer inference but merely a method to visualise the results for a population of galaxies (see appendix section C in Smethurst et al. 2016 for a discussion on alternative methods which may be used to determine the parent population SFH). These distributions will be referred to as the population SFH densities.

## 3 RESULTS

We determine the population SFH densities for both the regular and non-regular rotators of the Q-MANGA-GALEX sample. This is shown in Figure 3 for both the time that quenching occurs (left panel) and exponential rate of quenching

<sup>2</sup> Publicly available: <http://github.com/zoouniverse/starpy>

<sup>3</sup> <http://dan.iel.fm/emcee/>

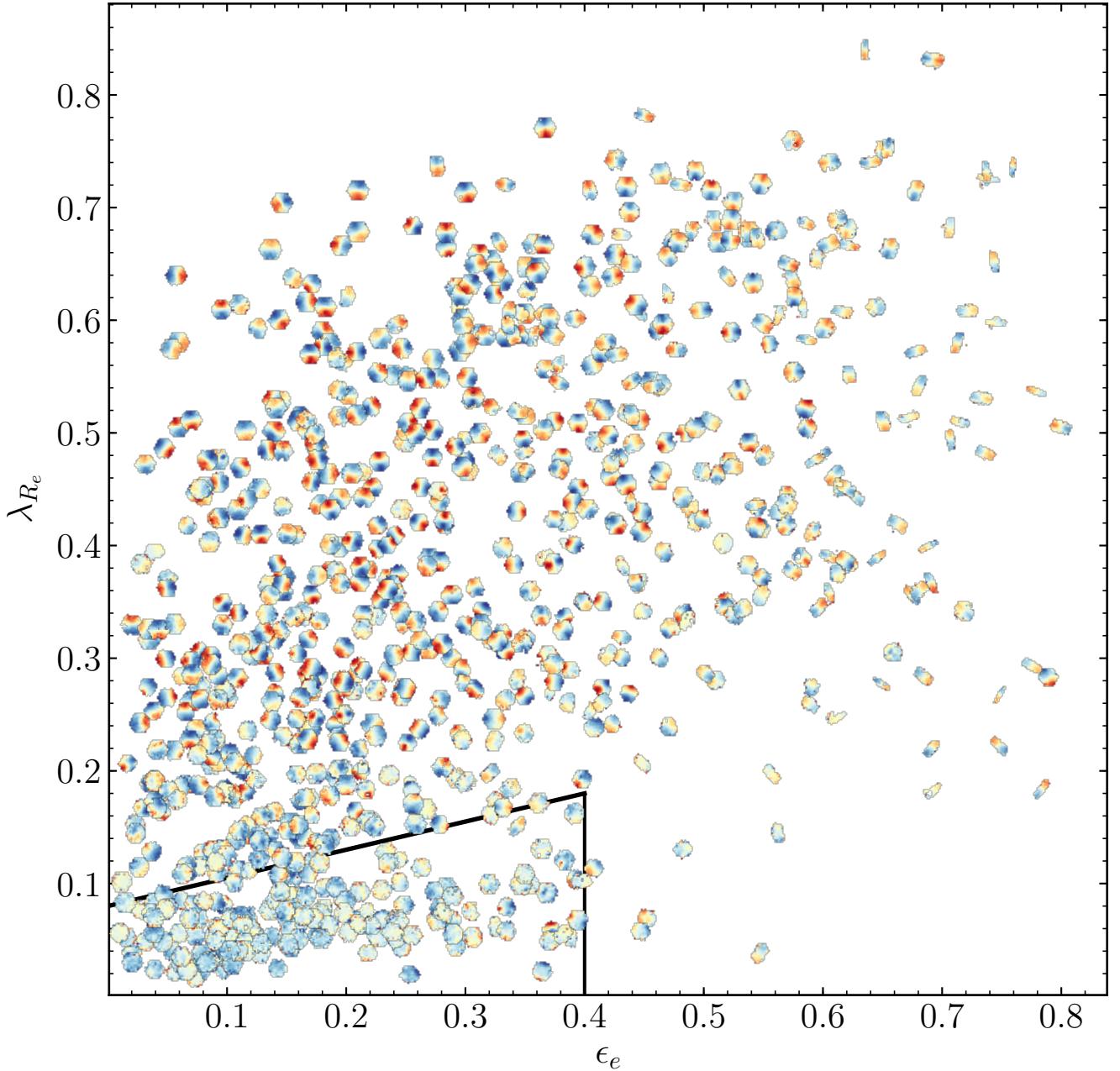


**Figure 2.** Ellipticity versus stellar angular momentum for the quenching and quenched galaxies in the current observed MaNGA sample. Each point is shown by its stellar velocity map, each normalised to have the midpoint, between maximum and minimum measured velocity dispersions, shown by the colour yellow. We show the separation between regular (i.e. fast) and non-regular (i.e. slow) rotators from Cappellari (2016) with the black solid line.

(right panel) in the regular (black solid line) and non-regular (red dashed line) rotator populations. Uncertainties on the population densities (shown by the shaded regions) are determined from the maximum and minimum values spanned by  $N = 1000$  bootstrap iterations, each sampling 90% of a either the regular (black shaded region) or non-regular (red shaded region) galaxy sample.

A Kolmogorov-Smirnov (KS) test was conducted first on the quenching time population densities (left panel of Figure 3) and revealed that we cannot reject the null hy-

pothesis that the regular and non-regular rotators quench at the same time ( $D \sim 0.17$ ,  $p \sim 0.09$ ). A second KS-test was conducted on the quenching rate population densities (right panel of Figure 3) and revealed that we can reject the null hypothesis that the fast and slow rotators quench at the same exponential rate ( $D \sim 0.27$ ,  $p \sim 0.0009$ ). This is a statistically significant ( $3\sigma$ ) result, suggesting that non-regular rotators are more likely to quench more rapidly than regular rotators.

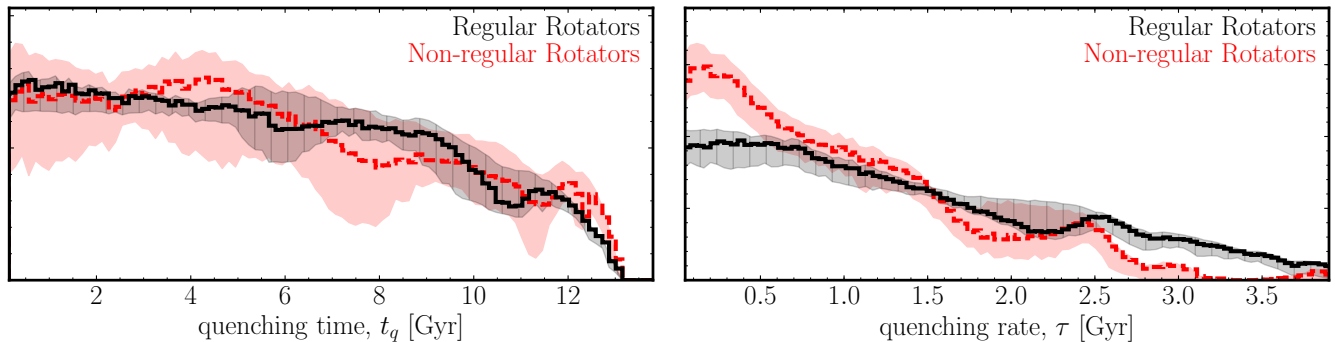


**Figure 3.** Population densities for the time,  $t_q$  (left) and exponential rate,  $\tau$  (right) that quenching occurs in the Q-MANGA-GALEX sample for regular (black, solid) and non-regular (red, dashed) rotators. A high value of  $t_q$  corresponds to a recent quench, and a high value of  $\tau$  corresponds to a slow quench. Shaded regions show the uncertainties on the distributions from bootstrapping. A KS-test between the  $t_q$  distributions revealed that we cannot reject ( $p = 0.09$ ) the null hypothesis that the regular and non-regular rotators quench at the same time. However, a KS-test between the  $\tau$  distributions revealed that we can reject ( $p = 0.0009$ ) the hypothesis that the regular and non-regular rotators quench at the same rate. This is a  $3\sigma$  result, suggesting that non-regular rotators quench more rapidly.

#### 4 DISCUSSION

The results shown in Figure 3 suggest that regular and non-regular rotators are indeed separate populations quenched, and therefore formed, by different mechanisms. However, these quenching mechanisms appear to occur at similar cosmic times for regular and non-regular rotators. However, STARPY is not very sensitive to the time of quenching, particularly at early times i.e.  $t_q \lesssim 6$  Gyr when  $z \gtrsim 1$ .

This explains the contradiction between our results and the simulations of Khochfar et al. (2011) who find that the last major merger interaction for slow rotators was at  $z \gtrsim 1.5$  (i.e.  $t_q \lesssim 4.5$  Gyr), whereas fast rotators continually accrete both stellar and gas mass through mergers and secular processes and so could be quenched at any epoch. Contradicting both the findings of Khochfar et al. (2011) and the results of this work, Penoyre et al. (2017) find in the Illustris simulation that slow rotators only form after  $z < 1$  (i.e.  $t_q \gtrsim 6$  Gyr).

Whilst the finding that regular rotators quench at all epochs, shown in the left panel of Figure 3, is in agreement with previous works, for the non-regular rotators we must question whether either (i) that STARPY is not sensitive enough to early quenching times to detect the epochs at which non-regular rotators quench (as in the Khochfar et al. 2011 picture) or (ii) the degeneracies of the SFH model result in the likelihood for quenching at early times for non-regular rotators when in fact they are quenching at late times (as in the Penoyre et al. 2017 picture).

We find that a fraction of the regular rotator sample quench at very slow rates ( $\tau \gtrsim 3$  Gyr; right panel of Figure 3). Since the Q-MANGA-GALEX sample has not been selected by visual morphology, there will be regular rotators which are disc dominated (i.e. with bulge-to-total mass ratios of less than 0.5 which would historically have been classified as a late-type galaxy). This likelihood for slower quenching rates is therefore likely to be caused by the effects of secular evolution through gas accretion, slowly quenching these disc galaxies off the SFS. Using the morphological classifications of Galaxy Zoo 2 (Lintott et al. 2011; Willett et al. 2013) we find that  $\sim 31\%$  of the regular rotators of the Q-MANGA-GALEX sample have a disc or featured debiased

vote fraction,  $p_d \geq 0.8$  (i.e. 80% of classifiers marked the galaxy as having either a disk or features), and a debiased merger vote fraction,  $p_{\text{merger}} < 0.223$  (i.e. is not currently undergoing a merger). This is consistent with the fact that  $26.0 \pm_{3.1}^{2.4}\%$  of the regular rotator quenching rate population density (black line in the right panel of Figure 3) is found at quenching rates  $\tau > 2$  Gyr. Conversely only  $\sim 5\%$  of the non-regular rotators were classified as having a disc or features, and of these galaxies 2/3 have a debiased odd vote fraction,  $p_{\text{odd}} \geq 0.3$ , suggesting they are undergoing either an interaction or merger.

The prevalence of rapid rates in the non-regular rotators of the Q-MANGA-GALEX sample supports the theory that these galaxies are formed by major mergers, which are thought to cause quenching at such rates (Springel et al. 2005; Bell et al. 2006; Lotz et al. 2008, 2011; Smethurst et al. 2015). However, we also find evidence for regular rotators quenching at these same rapid rates. Simulations have recently shown that although major mergers can cause rapid quenching of a galaxy, they do not necessarily destroy the disk dominated nature of a galaxy (Pontzen et al. 2016; Sparre & Springel 2016). This is thought to mainly occur in gas rich major mergers and is likely the explanation for the preference for rapid rates in the regular rotator sample seen in Figure 3.

Our results suggest that although the kinematics of regular and non-regular rotators are different in nature, the mechanisms which quench and therefore form these galaxies are very similar. However, in order to completely destroy the disk of a galaxy, some property in the formation/quenching mechanism must exceed some threshold. Since simulations have shown that it is possible for a disc to be retained in a major 1:1 mass ratio merger, this quantity cannot be the merger mass ratio as previously thought (Binney & Tremaine 1987; Bois et al. 2010; Tonini et al. 2016). Instead, our results showing similar quenching rates occurring across both regular and non-regular rotator samples, combined with the findings of recent simulations by Pontzen et al. (2016); Sparre & Springel (2016), suggest that the total gas mass within a pair of merging galaxies, is what will ultimately decide the kinematic fate of a galaxy.

## REFERENCES

- Abazajian K. N. et al., 2009, *ApJS*, 182, 543
- Bell E. F., Phleps S., Somerville R. S., Wolf C., Borch A., Meisenheimer K., 2006, *ApJ*, 652, 270
- Binney J., Tremaine S., 1987, *Galactic dynamics*
- Blanton M. R., Eisenstein D., Hogg D. W., Schlegel D. J., Brinkmann J., 2005, *ApJ*, 629, 143
- Blanton M. R., Roweis S., 2007, *AJ*, 133, 734
- Bois M. et al., 2010, *MNRAS*, 406, 2405
- Brinchmann J., Charlot S., White S. D. M., Tremonti C., Kauffmann G., Heckman T., Brinkmann J., 2004, *MNRAS*, 351, 1151
- Bruzual G., Charlot S., 2003, *MNRAS*, 344, 1000
- Bundy K. et al., 2015, *ApJ*, 798, 7
- Cappellari M., 2016, *ARA&A*, 54, 597
- Cappellari M. et al., 2007, *MNRAS*, 379, 418
- Cappellari M. et al., 2013, *MNRAS*, 432, 1862
- Cardelli J. A., Clayton G. C., Mathis J. S., 1989, *ApJ*, 345, 245
- Chabrier G., 2003, *PASP*, 115, 763
- Cheung E. et al., 2012, *ApJ*, 760, 131
- Drory N. et al., 2015, *AJ*, 149, 77
- Duc P.-A. et al., 2011, *MNRAS*, 417, 863
- Emsellem E. et al., 2011, *MNRAS*, 414, 888
- Emsellem E. et al., 2007, *MNRAS*, 379, 401
- Fang J. J., Faber S. M., Koo D. C., Dekel A., 2013, *ApJ*, 776, 63
- Foreman-Mackey D., Hogg D. W., Lang D., Goodman J., 2013, *PASP*, 125, 306
- Gunn J. E. et al., 2006, *AJ*, 131, 2332
- Hayward C. C., Torrey P., Springel V., Hernquist L., Vogelsberger M., 2014, *MNRAS*, 442, 1992
- Hopkins P. F., Cox T. J., Kereš D., Hernquist L., 2008a, *ApJS*, 175, 390
- Hopkins P. F., Hernquist L., Cox T. J., Di Matteo T., Robertson B., Springel V., 2006, *ApJS*, 163, 1
- Hopkins P. F., Hernquist L., Cox T. J., Kereš D., 2008b, *ApJS*, 175, 356
- Jarosik N. et al., 2011, *ApJS*, 192, 14
- Kauffmann G. et al., 2003, *MNRAS*, 341, 33
- Khochfar S. et al., 2011, *MNRAS*, 417, 845
- Khochfar S., Silk J., 2009, *MNRAS*, 397, 506
- Law D. R. et al., 2016, *AJ*, 152, 83
- Law D. R. et al., 2015, *AJ*, 150, 19
- Lintott C. et al., 2011, *MNRAS*, 410, 166
- Lotz J. M., Jonsson P., Cox T. J., Croton D., Primack J. R., Somerville R. S., Stewart K., 2011, *ApJ*, 742, 103
- Lotz J. M., Jonsson P., Cox T. J., Primack J. R., 2008, *MNRAS*, 391, 1137
- Martin D. C. et al., 2005, *ApJ*, 619, L1
- Martin D. C. et al., 2007, *ApJS*, 173, 342
- Mihos J. C., Hernquist L., 1994, *ApJ*, 431, L9
- Naab T. et al., 2014, *MNRAS*, 444, 3357
- Noeske K. G. et al., 2007, *ApJ*, 660, L43
- Oh K., Sarzi M., Schawinski K., Yi S. K., 2011, *ApJS*, 195, 13
- Padmanabhan N. et al., 2008, *ApJ*, 674, 1217
- Peng Y.-j. et al., 2010, *ApJ*, 721, 193
- Penoyre Z., Moster B. P., Sijacki D., Genel S., 2017, *ArXiv e-prints*, 1703.00545
- Pontzen A., Tremmel M., Roth N., Peiris H. V., Saintonge A., Volonteri M., Quinn T., Governato F., 2016, *ArXiv e-prints*, 1607.02507
- Schawinski K. et al., 2014, *MNRAS*, 440, 889
- Smee S. A. et al., 2013, *AJ*, 146, 32
- Smethurst R. J. et al., 2017, *MNRAS*
- Smethurst R. J. et al., 2016, *MNRAS*, 463, 2986
- Smethurst R. J. et al., 2015, *MNRAS*, 450, 435
- Snyder G. F., Cox T. J., Hayward C. C., Hernquist L., Jonsson P., 2011, *ApJ*, 741, 77
- Sparre M., Springel V., 2016, *ArXiv e-prints*, 1610.03850
- Springel V., Di Matteo T., Hernquist L., 2005, *ApJ*, 620, L79
- Stott J. P. et al., 2016, *MNRAS*, 457, 1888
- Stoughton C. et al., 2002, *AJ*, 123, 485
- Tonini C., Mutch S. J., Croton D. J., Wyithe J. S. B., 2016, *MNRAS*, 459, 4109
- Toomre A., Toomre J., 1972, *ApJ*, 178, 623
- Weiner B. J. et al., 2006, *ApJ*, 653, 1049
- Willett K. W. et al., 2013, *MNRAS*, 435, 2835
- Yan R. et al., 2016, *AJ*, 152, 197
- York D. G. et al., 2000, *AJ*, 120, 1579